Research progress of performance optimization of tunnel magnetoresistive sensors*

LIU Yuanzhen[1], LEI Shaoyu[1], ZHANG Shiyi[1], PAN Mengchun[1, 2], HU Yueguo[1, 2], HU Jiafei[1, 2], PENG Junping[1, 2], DU Qingfa[1, 2], ZHANG Qi[1, 2], LI Peisen[1, 2, *]

1. College of Intelligence Science and Technology, National University of Defense Technology, Changsha 410073, China
2. National Key Laboratory of Equipment State Sensing and Smart Support, National University of Defense Technology, Changsha 410073, China

Abstract

Tunnel magnetoresistance (TMR) sensors have emerged as a leading technology in high-performance magnetic sensing due to their high sensitivity, low power consumption, and miniaturization. In order to meet the everchanging demands of cutting-edge applications such as biomagnetic imaging and smart grid monitoring, continuous performance enhancement is crucial. This paper systematically reviews the key strategies for optimizing TMR sensors, focusing on thin-film material engineering and sensitive microstructure design. Material advancements are dissected along two paths: developing high-sensitivity systems via MgO barriers and composite free layers, and creating wide-linear-range systems through anisotropy engineering, including both perpendicular (PMA) and in-plane (IMA) configurations, as well as dynamic methods such as electric-field and strain modulation. Structurally, we highlight innovations such as vortex-state magnetic tunnel junctions (MTJs) and magnetic flux concentrators to enhance linearity and sensitivity, as well as advanced noise modulation techniques that effectively suppress low-frequency 1/*f* noise. The practical effect of these optimizations is reflected in the fact that TMR sensors can now measure magnetocardiograms (MCG) outside shielded environments and provide high-accuracy current sensing in smart grids. The future development is directed toward novel material systems that pursue either enhanced sensitivity or an extended linear range, the realization of monolithic three-axis vector sensors, and the deep

* The paper is an English translated version of the original Chinese paper published in Acta Physica Sinica. Please cite the paper as: LIU Yuanzhen[1], LEI Shaoyu[1], ZHANG Shiyi[1], PAN Mengchun[1, 2], HU Yueguo[1, 2], HU Jiafei[1, 2], PENG Junping[1, 2], DU Qingfa[1, 2], ZHANG Qi[1, 2], LI Peisen[1, 2, *], **Research progress of performance optimization of tunnel magnetoresistive sensors**. *Acta Phys. Sin.*, 2026, 75(6):060803. doi: 10.7498/aps.75.20251597

integration of TMR technology with artificial intelligence for smart sensing systems. This work provides a comprehensive reference for advancing TMR sensor technology and its applications in high-precision magnetic field detection.

Keywords：tunneling magnetoresistance magnetic sensor; performance optimization; thin film material; magnetic tunnel junction structure design

DOI: 10.7498/aps.75.20251597

CSTR: 32037.14.aps.75.20251597

1 Introduction

With the rapid development of emerging technologies such as the Internet of Things (IoT), artificial intelligence (AI), new energy vehicles, and embodied intelligence, sensors, serving as the "nerve endings" for information perception, are experiencing unprecedented opportunities. In recent years, driven by strategic emerging industries including industrial automation, intelligent manufacturing, and new energy vehicles, magnetic sensors have become core components of the intelligent perception layer. This prominence stems from their non-contact measurement capabilities, high reliability, and excellent adaptability to complex environments, leading to continuous expansion of the global market. Currently, the chip-level magnetic sensor market is dominated by Hall sensors and magnetoresistive sensors[1]. Hall sensors hold the majority market share due to advantages such as small size, low cost, and mature manufacturing processes. However, with the advancement of smart grids, new energy vehicles, and robotics, the sensitivity and frequency response of existing Hall sensors increasingly fail to meet the timely, safe, and reliable requirements of new technologies. In contrast, magnetoresistive sensors are receiving growing attention from both academia and industry due to their high sensitivity, low power consumption, and wide frequency response. Magnetoresistive sensors are primarily categorized into anisotropic magnetoresistance (AMR) sensors, giant magnetoresistance (GMR) sensors, and tunneling magnetoresistance (TMR) sensors. Table 1 summarizes the key performance indicators of these magnetic sensors. It is evident that TMR sensors offer more significant advantages in high sensitivity, low power consumption, and miniaturization compared to AMR and GMR sensors. Consequently, TMR sensors have become a focal point of current research and a crucial technical pathway for the industry to develop high-performance, miniaturized magnetic sensing solutions[1,2].

Table 1 Comparison of typical performance metrics for magnetic sensors.

Performance	Hall	MR		
		AMR	GMR	TMR
Maximum magnetoresistance ratio/%	/	2	24	631
Magnetic field sensitivity/(%·Oe-1)	1	~1	~3	~100
Resolution/(nT·Hz-1/2)	130	~1	~10	~0.01
Power consumption/mW	35	~29	~110	~0.07
Chip size	Larger	Medium	Medium	Smaller
Frequency response range	DC-100 kHz	DC-1 MHz	DC-1 MHz	DC-several MHz

Tunneling magnetoresistance (TMR) magnetic sensors represent a new generation of spintronic devices based on the tunneling magnetoresistance effect. Their physical essence stems from spin-dependent quantum tunneling behavior exhibited by electrons within nanoscale insulating barrier layers. French scholar Julliere[3] first discovered the TMR effect in Fe/Ge-O/Co multilayer films in 1975. Due to their high reliability and sensitivity, these devices were initially widely applied in hard disk drive read heads. In 2014, TDK launched the world's first TMR chip designed for sensor applications. This milestone marked the expansion of the technology from data storage to sensing scenarios such as current and position detection. Benefiting from high sensitivity, low power consumption, miniaturization, and excellent stability, TMR sensors have rapidly gained recognition in the automotive, industrial, and new energy sectors in recent years, ushering in vigorous technological development. However, existing TMR sensors still face severe challenges in enhancing sensitivity, suppressing low-frequency noise, improving resolution, and extending the linear dynamic range. These challenges persist despite emerging demands in fields such as biomagnetic detection, space magnetic field measurement, high-precision industrial automation control, and smart grid monitoring[4-6]. To overcome these bottlenecks, current research focuses on synergistic innovations in two key areas. On one hand, researchers optimize performance metrics such as sensitivity, noise, and dynamic range by refining thin-film material systems. On the other hand, they pursue further performance breakthroughs through innovative designs of the magnetic tunnel junction (MTJ) sensing structure. This article addresses these two critical aspects. After introducing the evolution of the basic structure of TMR magnetic sensors and the evaluation system for performance metrics, we summarize optimization strategies for thin-film material systems. We also outline approaches to enhance sensor performance through magnetic tunnel junctions (MTJ) structure design. Finally, we discuss the prospects for the application prospects and development challenges of TMR magnetic sensors.

2 Basic Physical Structure

The core structure of a TMR sensor typically consists of a "ferromagnetic layer/insulating barrier layer/ferromagnetic layer" stack, as shown in Figure 1, forming a sandwich-like configuration. The magnetization direction of one ferromagnetic layer is pinned (referred to as the reference layer), while the other serves as a free layer that can rotate freely in response to an external magnetic field. According to the TMR effect, when the magnetization directions of the two ferromagnetic layers are parallel, majority spin electrons from one layer can tunnel into the majority spin empty states of the other layer. Simultaneously, minority spin electrons tunnel into the corresponding minority spin empty states. This results in a high overall tunneling probability, manifesting as a low resistance state R_P. Conversely, when the magnetization directions are antiparallel, majority spin electrons from one layer tunnel into the minority spin empty states of the other layer. This leads to a significant increase in resistance, resulting in a high resistance state R_{AP}. The parameter used to quantify the extent of this resistance change is known as the tunneling magnetoresistance ratio (TMR ratio), defined as

$$\mathrm{TMR} = \frac{R_{AP} - R_P}{R_P} \times 100\%. \quad (1)$$

The fundamental functional unit of a TMR sensor is the magnetic tunnel junction (MTJ). Its basic structure comprises a buffer layer, an antiferromagnetic layer, a reference layer, a barrier layer, a free layer, and a capping layer. The buffer layer resides at the bottom of the thin film. It induces structural orientation in key layers to enhance the TMR ratio. Additionally, increasing its thickness reduces the wiring resistance of the MTJ, thereby further improving the TMR value. Common buffer materials employ a multilayer Ru/Ta composite structure. The antiferromagnetic layer primarily functions to pin the magnetic moment of the reference layer in a fixed direction through high-temperature magnetic annealing. This process leverages the strong exchange bias interaction between the ferromagnetic and antiferromagnetic layers, rendering the MTJ a uniaxial magnetic sensor. The reference layer consists of a synthetic antiferromagnetic structure. This structure includes two ferromagnetic layers coupled antiparallel via a non-magnetic spacer layer. Such a configuration effectively minimizes the influence of stray fields on the free layer while ensuring excellent stability for the MTJ. The free layer detects the external magnetic field variations. Its magnetic moment rotates controllably under an applied magnetic field. This rotation alters the relative orientation angle with respect to the reference layer. Consequently, the tunneling magnetoresistance effect converts magnetic field information into measurable resistance change signals. Early studies predominantly employed a "single-pinning" system that fixed only the reference layer's magnetic moment[7,8]. Although this approach offers simple processing, the free layer is prone to hysteresis during magnetic response, leading to nonlinear output signals. To overcome these limitations, researchers developed a "double-pinning" system. This design introduces antiferromagnetic layers with different blocking temperatures to the free and reference layers, respectively[9,10]. This arrangement allows controlled pinning strength and direction for both magnetic layers under specific annealing processes. It effectively balances the anisotropy and thermal stability of the free layer. As application scenarios become increasingly complex and diverse, performance requirements for TMR magnetic sensors have become more stringent. Consequently, the structural complexity of TMR thin-film materials has increased.

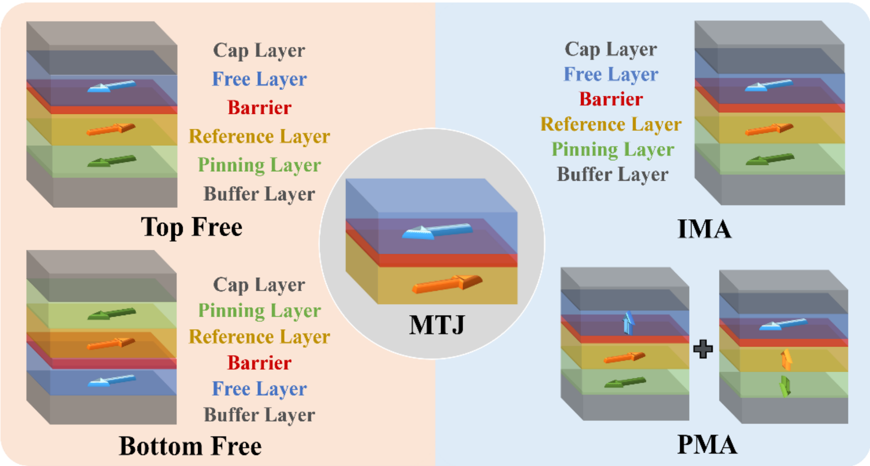

Fig. 1 Schematic of the basic structure and classification of MTJs: (a) Classification based on the position of the free layer; (b) classification based on anisotropy directions.

Based on the position of the free layer, MTJs are classified into two basic configurations: "bottom-free" and "top-free," as shown in Figure 1(a). In the bottom-free configuration, the free layer is located at the bottom of the material stack. This arrangement facilitates high-quality crystallization at the bottom interface. It also enables optimization of structural dimensions to achieve consistent magnetic moment switching and effectively suppress noise[11]. While this configuration demonstrates superior stability in sensor applications, it presents new challenges for the growth of pinning structures. In the top-free configuration, the free layer is positioned at the top of the material stack. This approach benefits from mature thin-film growth processes. Furthermore, it allows precise control of shape anisotropy through patterning techniques and facilitates the integration of magnetic flux concentrators (MFCs). These features significantly enhance the response to external magnetic fields, making the top-free configuration the mainstream technical solution for TMR magnetic sensing.

Additionally, MTJs are categorized into in-plane magnetic anisotropy (IMA) and perpendicular magnetic anisotropy (PMA) types based on the direction of magnetic anisotropy[12], as illustrated in Figure 1(b). IMA-MTJs primarily rely on shape anisotropy generated by the device's aspect ratio to stabilize the magnetization direction. They combine high TMR values with low noise characteristics and are widely used in high-sensitivity magnetic field sensors. In contrast, PMA-MTJs induce magnetization perpendicular to the film plane through specific material systems (such as $L1_0$-phase FePt or CoPt alloys) or strong interface effects (such as the CoFeB/MgO interface). This configuration achieves a wider linear magnetic field range and lower nonlinearity. It also offers superior scalability and thermal stability, making it particularly suitable for magnetic sensors requiring high temperature stability and a wide dynamic range. These two major configurations and their variants form the foundation of modern TMR devices. Their performance can be finely tuned through material selection, post-processing techniques, and structural design to meet the demands of various application scenarios.

3 Performance Optimization

3.1 Performance Metrics

Multiple metrics collectively evaluate the performance of TMR magnetic sensors. A comprehensive analysis of the physical definitions, formation mechanisms, and optimization pathways for these metrics requires considering the magnetic sensitivity mechanism of the MTJ, material characteristics, and fabrication processes[13-15]. Figure 2 displays the magnetoresistance response curve and the noise spectral density curve of a TMR magnetic sensor. These curves reflect several key performance indicators of the TMR magnetic sensor, which are detailed below.

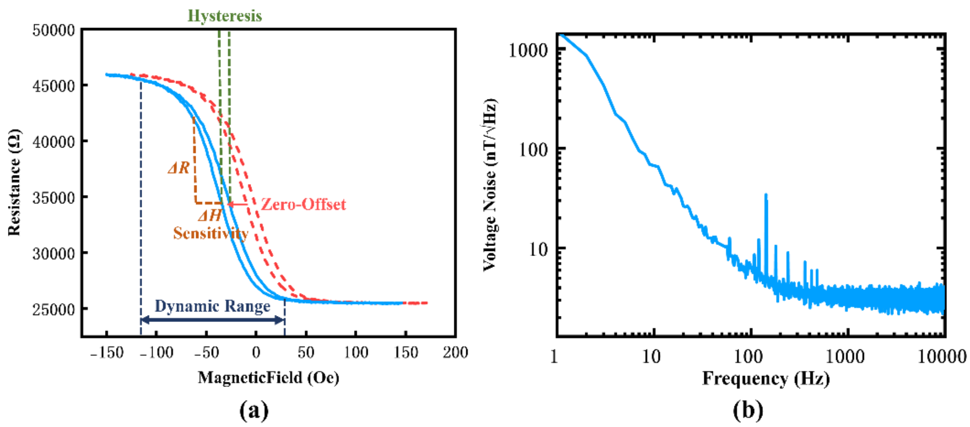

Fig. 2 Schematic diagram of performance indicators: (a) Magnetoresistance response curve; (b) Noise spectral density curve

1) Measurement Range: This refers to the range of external magnetic field variations that a TMR magnetic sensor can detect and measure accurately. Ideally, the TMR measurement range corresponds to the difference in magnetic field strength required to drive the MTJ unit into parallel and antiparallel states. Based on the free energy analysis of the MTJ, the equivalent anisotropy field H_k of the free layer is the key determinant of the measurement range. A larger H_k requires a stronger external magnetic field for the free layer magnetic moment to overcome anisotropy energy and switch, thereby resulting in a wider measurement range. Therefore, optimizing the measurement range typically focuses on regulating the anisotropy field.

2) Sensitivity: Sensitivity is a core parameter measuring the sensor's response capability to external magnetic fields. It is typically defined as the relative change rate of resistance per unit change in magnetic field within the linear range of the measurement range. Physically, it represents the combined effect of the reversible rotation degree of the free layer magnetic moment under an external magnetic field and the tunneling magnetoresistance effect. Mechanistically, the MTJ resistance varies with the angle between the magnetic moments of the free layer and the reference layer. When an external magnetic field drives the rotation of the free layer magnetic moment, the change in this angle alters the tunneling resistance. A higher TMR value and a smaller equivalent anisotropy field result in more significant resistance changes per unit magnetic field, thus yielding higher sensitivity. Regarding optimization, material systems with high TMR values and optimized magnetic anisotropy designs can significantly enhance sensitivity. Furthermore, structural designs such as introducing flux concentrators or employing multi-junction series connections can effectively boost sensitivity. However, improving sensitivity requires trade-offs with parameters such as measurement range and hysteresis. Excessively high sensitivity may lead to an overly small saturation field, thereby limiting the dynamic measurement range.

3) Hysteresis: Hysteresis manifests as the non-coincidence of the magnetoresistance response curves during increasing and decreasing magnetic field processes. The coercivity metric is used to quantify the hysteresis level of the MTJ. Hysteresis primarily stems from the irreversibility of the free layer magnetization process. This includes irreversible magnetization processes such as domain wall pinning sites within the material, magnetic domain splitting caused by anisotropy inhomogeneity, and Néel coupling between the reference and free layers. The presence of hysteresis introduces measurement errors, severely affecting precision, particularly in weak field and alternating magnetic field detection. Suppressing hysteresis requires improving magnetization reversibility. Strategies include optimizing the soft magnetic properties of materials, introducing exchange bias fields to stabilize magnetic moment orientation, and enhancing internal uniaxial anisotropy.

4) Zero-Bias Offset: Zero-bias offset refers to the degree to which the linear region of the magnetic sensitive element's response curve deviates from the zero magnetic field. It is defined as the midpoint of the magnetic field within the measurement range. For a single MTJ unit, zero-bias offset mainly arises from asymmetry in the internal unidirectional anisotropy field. Factors include the Néel coupling field between the reference and free layers, and deviations in the direction of the exchange bias field exerted by the antiferromagnetic layer on the free layer after secondary annealing. Additionally, inconsistencies among the four bridge arm MTJs in a sensor bridge structure can further exacerbate the zero-bias offset. This leads to sensitivity attenuation near the zero field, affecting weak field measurement precision. Therefore, optimizing zero-bias offset performance can involve compensating for the internal bias field of the MTJ and improving the consistency of devices within the bridge structure.

5) Noise: Noise refers to random signals in the sensor output that are unrelated to the measured physical quantity. It is a key factor limiting the ultimate detection precision of the sensor. As a tunneling electronic device, MTJ noise includes not only electrical noise caused by material defects and thermal disturbances in electronic components but also magnetic-related noise induced by thermal fluctuations of magnetic moments. Typically, TMR background noise is categorized in the frequency domain into white noise, which is independent of frequency, and $1/f$ noise, which is frequency-dependent.

6) Resolution: As a comprehensive indicator reflecting the minimum detectable magnetic field change of the sensor, resolution is theoretically defined as

$$D = \frac{\sqrt{S_V}}{SV}. \quad (2)$$

In this equation, $\sqrt{S_V}$ represents the voltage spectral density of noise, S denotes sensitivity, and V indicates the operating voltage. The unit of D is typically $pT/\sqrt{Hz}$. Its performance upper limit depends not only on the synergistic optimization of sensitivity and noise but is also indirectly influenced by nonlinear factors such as hysteresis and zero-bias offset. Excessive hysteresis causes inconsistent output during magnetic field cycling, while zero-bias drift reduces effective sensitivity near the zero-field region. Both factors degrade the actual resolution. Therefore, resolution reflects the comprehensive performance of TMR sensors. It serves as a key metric for evaluating TMR sensor quality, requiring the coordinated consideration of multiple factors during performance optimization.

Table 2 summarizes the core performance metrics of TMR sensors developed by various research teams[16-22]. In addition to the aforementioned core metrics, frequency response and thermal stability are also critical indicators for assessing the overall performance of TMR magnetic sensors. Frequency response characterizes the ability of

TMR sensors to respond to alternating magnetic fields. Its upper limit is primarily constrained by the ferromagnetic resonance frequency of the MTJ materials and the distributed parameters formed by parasitic capacitance and inductance in the readout circuit[23]. These factors collectively determine the high-frequency cutoff point of the sensor. Optimizing frequency response requires approaches from both material and structural perspectives. For instance, one may employ materials with high anisotropy fields to increase the intrinsic resonance frequency. Alternatively, reducing junction dimensions and optimizing electrode layouts can minimize parasitic effects. Thermal stability reflects the ability of sensor performance parameters to remain stable under varying environmental temperatures. This stability is rooted in the temperature-dependent intrinsic magnetic properties of the ferromagnetic and barrier layers constituting the tunnel junction, such as saturation magnetization and anisotropy constants. Furthermore, factors like interfacial atomic diffusion and thermal stress can induce irreversible drift during temperature cycling. Strategies to enhance thermal stability include selecting magnetic material systems with superior temperature coefficients and introducing temperature compensation mechanisms at the circuit level. These measures help maintain stable sensor performance across a wide temperature range.

Table 2 Comparison of TMR sensor performance indicators among various research teams.

Research Team	Range /Oe	Sensitivity/(mV·V-1·Oe -1)	Hysteresis/ Oe	Noise/(nV·Hz-1/ 2)	Resolution/(pT·Hz-1 /2)
Tohoku University, Japan[16]	/	1150	1	/	0.94(@1 Hz)
Brown University, USA[17]	±20	28	~0	/	/
INESC MN, Portugal[18]	/	1860	/	6.24(@10 Hz)	49(@10 Hz)
Beihang University[19]	100	1.57	/	/	29.3×10^3(@10 Hz)
University of Chinese Academy of Sciences[20]	/	22.29	/	6.3	300(@1 kHz)

Institute of Physics, Chinese Academy of Sciences[21]	50	10.7	/	/	10×10^3(@1 Hz)
National University of Defense Technology	±15	16.38	0.006	121.97	740
Xi'an Jiaotong University[22]	±20	6	~0	/	/

3.2 Optimization of Thin-Film Material Systems

3.2.1 High-Sensitivity TMR Material Systems

The development of high-sensitivity tunneling magnetoresistance (TMR) material systems originated from the need for weak magnetic field detection. As shown in Figure 3, this evolution primarily follows two optimization pathways. The first focuses on optimizing the barrier layer to increase the TMR ratio, thereby enhancing device sensitivity. The second targets the free layer to achieve rapid, low-loss magnetic response while effectively suppressing device noise within the linear operating range.

1) Optimization of Barrier Layer Materials

Optimizing the barrier layer aims to enhance spin-dependent electron tunneling probability. This approach seeks to achieve an order-of-magnitude breakthrough in TMR values, thereby attaining ultra-high sensitivity. In 1975, Julliere[3] first observed the TMR effect in low-temperature Fe/GeO/Co junctions. However, technical limitations at the time prevented the reproduction of this phenomenon for a long period. It was not until the late 1990s that room-temperature TMR was rediscovered in amorphous Al-O-based magnetic tunnel junctions (MTJs), attracting widespread attention[24,25]. Nevertheless, despite continuous process improvements, the room-temperature TMR values of amorphous Al-O systems remained around 80%. This level failed to meet the requirements for high-sensitivity sensing applications.

In 2001, Butler et al.[26] predicted through first-principles calculations that TMR values could exceed 1000% in MTJs with (001)-oriented MgO barriers. This finding significantly boosted researcher confidence in MgO-based tunnel junctions. In 2004, Yuasa et al.[27] successfully fabricated MgO-based MTJs using molecular beam epitaxy, achieving a room-temperature TMR of 180%. In the same year, IBM reported a TMR value as high as 410%[28], marking the formal rise of MgO-based systems. In 2008, Ikeda et al.[29] obtained a room-temperature TMR of 604% in CoFeB/MgO/CoFeB structures through high-temperature annealing. This result fully verified the significant advantages of MgO over Al-O. In 2023, Scheike et al. from the National Institute for Materials Science in Japan[30] pushed the room-temperature TMR to 631% using CoFe/Mg interface interlayer technology, reaching the world's highest level. However, ultra-high TMR materials have not yet been widely used in sensors due to issues such as magnetic property matching. Currently, the TMR values of practical MTJs mostly remain in the 150%-240% range, indicating that performance improvements in MgO systems are approaching a bottleneck.

In this context, exploring new barrier layer materials has become a new direction. Graphene is regarded as a highly promising candidate due to its atomic-level flatness, ultra-high carrier mobility, and long spin diffusion length[31]. Karpan et al. from the University of Twente in the Netherlands[32] and the research group of Pan Mengchun at the National University of Defense Technology[33] analyzed the feasibility of graphene-based tunnel junctions using first-principles calculations. They found that ferromagnet/graphene interfaces produce a perfect spin filtering effect, thereby yielding an extremely high magnetoresistance change rate. Furthermore, two-dimensional materials such as hexagonal boron nitride and transition metal dichalcogenides can effectively suppress lattice mismatch and interface scattering through van der Waals interfaces. This significantly enhances tunneling efficiency[34,35]. Although new materials like graphene still face challenges in fabrication processes and interface control, their unique physical properties and vast potential for performance optimization make them an important development direction for barrier layers in future high-TMR devices.

2) Optimization of Free Layer Materials

At present, the extent of TMR value improvement achievable through barrier layer optimization is limited. In contrast, starting with the optimization of soft magnetic properties to reduce the saturation field of the sensing element offers a more promising path for significantly enhancing sensitivity. In 2012, Fujiwara et al. from Tohoku University in Japan[36] employed a composite free layer with a CoFeB/Ru/NiFe structure. They utilized the NiFe layer, which has a lower anisotropy field, to drive the magnetic moment rotation of the CoFeB layer, thereby reducing the overall saturation magnetic field of the free layer. By using a thicker NiFe layer (70 nm), they achieved a sensitivity of 25.3%/Oe in devices with an aspect ratio of 2. This performance is sufficient for use as a high-sensitivity magnetic field sensor. In 2013, this team grew the composite free layer beneath the magnesium oxide to ensure a more intact free layer during MTJ fabrication. This approach reduced the effective anisotropy of the free layer to enhance sensitivity and lowered noise by increasing the free layer area[11]. Additionally, they attempted to use the new soft magnetic material CoFeSiB to form a composite free layer. By leveraging the low coercivity and high crystallization temperature of CoFeSiB, they improved the soft magnetic properties of the device after annealing, achieving a maximum sensitivity of 40%/Oe[11]. Moreover, the amorphous CoFeSiB lacks grain boundaries, resulting in a flatter surface. This significantly reduces 1/*f* noise without affecting the lattice matching between CoFeB and MgO[37]. Since 2015, Tohoku University and the Institute of Physics, Chinese Academy of Sciences, have collaborated to continuously optimize designs based on thick NiFe or CoFeSiB free layers. They investigated the optimal free layer design by varying factors such as free layer thickness, interlayer materials, and antiferromagnetic layer thickness. They developed two types of high-sensitivity TMR materials featuring 70 nm thick NiFe and 140 nm CoFeSiB free layers, respectively. The device sensitivity achieved with the CoFeSiB free layer TMR film reached 1150%/mT, setting a new world record[38-42]. In 2023, Matos et al.[43] further optimized the soft magnetic properties and TMR values by adjusting the thickness and material of the interlayer within the composite free layer. They compared the magnetic properties of free layer materials such as CoFeBTa and CoFeSiB and increased the annealing temperature. Composite free layers with thick soft magnetic materials represent an important development trend for high-sensitivity TMR films. However, thick free layers can introduce issues such as multi-domain formation and hysteresis, which degrade the sensing performance of MTJs. Therefore, further optimization of composite free layer material design is required to achieve performance breakthroughs.

In addition to optimizing soft magnetic materials composite with CoFeB, researchers have also attempted to replace CoFeB with other materials that possess high TMR potential and excellent soft magnetic properties. The goal is to obtain better magnetic performance while maintaining the quality of the barrier layer interface. For instance, new materials such as FeAlSi and Heusler alloys have been introduced into the free layer to seek new breakthroughs. The ordered structure of FeAlSi itself brings its magnetocrystalline anisotropy close to zero, resulting in very low anisotropy, which makes it suitable as a high-sensitivity free layer material. However, this material has extremely high requirements for deposition processes and is easily oxidized by MgO[44,45]. Furthermore, using Heusler alloys with extremely high spin polarization is another approach. However, achieving a highly ordered structure within the TMR thin-film system faces complex growth process challenges. Additionally, the MgO interface can disrupt its half-metallic nature[46,47]. The TMR values of magnetic tunnel junctions fabricated with these new materials reach a maximum of only 121%[45]. There remains significant room for improvement, and the complex process challenges make it difficult to revolutionize high-sensitivity TMR material systems in the short term.

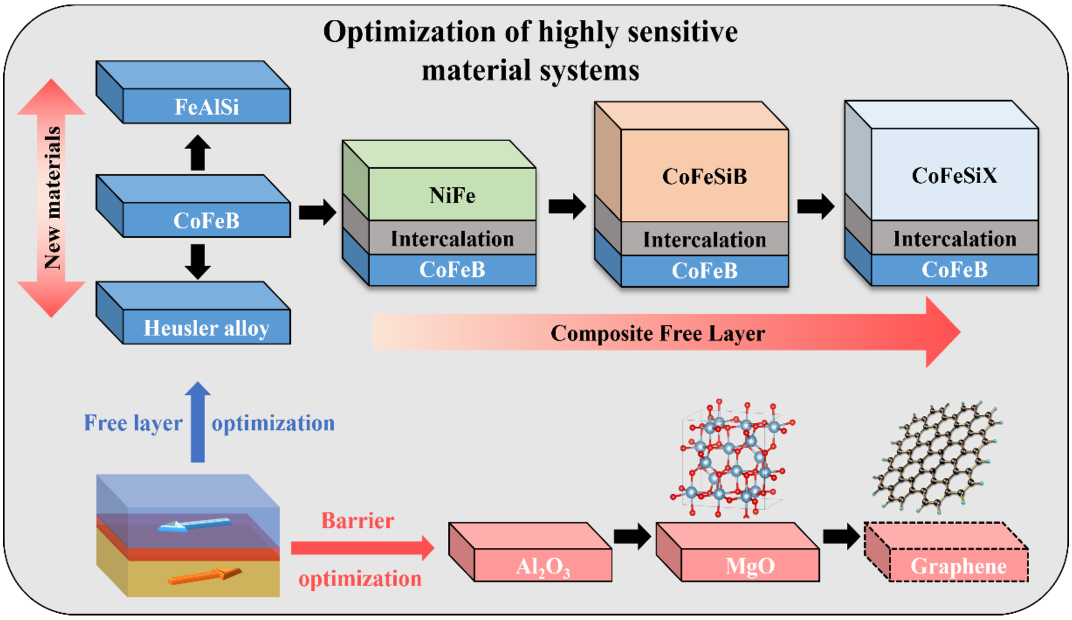

Fig. 3 Optimization approaches for free-layer materials

3.2.2 Wide-Range TMR Material Systems

The development of wide-range tunneling magnetoresistance (TMR) material systems stems from the demand for high-precision magnetic measurements in environments with large-scale, strong magnetic fields, such as smart grids, new energy vehicles, and industrial automation. The core objective is to significantly expand the linear measurement range of TMR sensors at the material system level. This material system primarily employs static modulation of magnetic anisotropy, extending to dynamic range expansion methods such as strain modulation and electric field modulation, as shown in Figure 4.

Wide-range material systems based on perpendicular magnetic anisotropy (PMA) represent the current mainstream technology. By constructing PMA magnetic tunnel junctions (MTJs), the magnetic moment of the reference layer is oriented perpendicular to the film plane. PMA generation relies mainly on two mechanisms. The first is intrinsic crystal anisotropy. For instance, using $L1_0$-phase FePt and CoPt alloys as the free layer provides high inherent PMA strength, widening the linear range to the kOe level. In 2017, Zhao et al.[48] used vertically magnetized $L1_0$-MnGa alloys as the reference layer. They achieved a TMR value of up to 27.4% at room temperature and an extremely wide dynamic range of 5600 Oe. This fully demonstrated the application potential of $L1_0$-phase alloys in wide-range TMR devices. The second mechanism is interface-induced anisotropy, typically represented by the CoFeB/MgO/CoFeB system.

Significant PMA arises at the interface through spin-orbit coupling effects between the ultrathin CoFeB layer and the MgO barrier, combined with designs such as artificially synthesized antiferromagnets (SAF). In 2012, Zeng et al.[49] used CoFeB materials with interface perpendicular anisotropy as the free layer. They constructed nanoscale MTJ sensors with in-plane magnetized reference layers. This configuration achieved a magnetic field sensitivity of up to 0.0017%/Oe and a wide linear measurement range exceeding 600 Oe. These results fully demonstrated the potential of perpendicular anisotropy CoFeB in nanoscale, high-sensitivity, low-power magnetic sensors. Building on this, Nakano's team at Tohoku University in Japan conducted systematic research on CoFeB/MgO-based PMA-MTJs. They further revealed the inherent trade-off between sensitivity and nonlinearity in this material system and significantly expanded the device dynamic range through material system design. In 2015, the team[50] systematically adjusted parameters for MTJs with perpendicular magnetic anisotropy CoFeB free layers, based on the Stoner-Wohlfarth model. By varying the thickness and Fe content of the CoFeB free layer, they effectively modulated the anisotropy field H_k. Experimental results clearly verified a constraint relationship between sensitivity and nonlinearity dominated by H_k: a smaller H_k yields higher sensitivity but greater nonlinearity, and vice versa. Under optimized conditions, they achieved a sensitivity as high as 0.048%/Oe (corresponding to 5.5% FS nonlinearity) and nonlinearity as low as 0.4% FS (corresponding to 0.004%/Oe sensitivity) within a ±400 Oe linear sensing range. To further break through dynamic range limitations, the team[51] upgraded the reference layer to a vertical synthetic antiferromagnetic (p-SAF) structure based on [Co/Pd] in 2017. By utilizing the exchange bias field generated by strong antiferromagnetic coupling, they successfully extended the linear response range to over ±2 kOe. This provided a feasible technical path for the design of CoFeB/MgO-based PMA-MTJ material systems. The core advantage of PMA structures lies in significantly enhanced magnetic anisotropy. This makes the flipping process of the free layer magnetic moment smoother, thereby substantially widening the linear response interval. Meanwhile, the higher thermal activation energy barrier effectively improves thermal stability of the device in the wide temperature range of -40 to 150 ℃, meeting the application requirements of harsh industrial environments[52]. However, PMA-MTJs still exhibit two key defects in practical applications. First, achieving a wide dynamic range often accompanies a significant drop in sensitivity. This requires comprehensive trade-offs and optimized design by finely tuning parameters such as the effective anisotropy field of the free layer, barrier layer quality, and TMR value. Second, the magnetic moment orientation of the reference layer based on perpendicular anisotropy cannot be stably pinned via antiferromagnetic coupling. When external strong magnetic field interference exceeds a certain range, the reference layer magnetic moment will flip, preventing accurate measurement of the external magnetic field.

In contrast, wide-range material systems with in-plane anisotropy have a limited range expansion capability. However, they maintain a high level of sensitivity and can achieve stable pinning of the reference layer magnetic moment through antiferromagnetic coupling, offering strong anti-interference capabilities. Typical strategies for widening the range in in-plane anisotropy material systems include: flexibly setting the linear operating interval by precisely controlling the CoFeB free layer thickness and its effective anisotropy field; introducing in-plane uniaxial anisotropy via oblique sputtering deposition[53]; or suppressing abrupt magnetic flipping to extend the linear response range using methods such as artificial defect engineering[54]. These methods are suitable for industrial sensing scenarios with medium-to-high ranges and cost sensitivity, achieving a certain degree of range expansion while maintaining high sensitivity.

In addition to the aforementioned static range control methods, dynamic range adjustment technologies have made significant progress in recent years, substantially improving the adaptability and intelligence level of TMR sensors. Dynamic range adjustment technologies mainly include electric field control and stress control. Electric field control introduces effects such as voltage-controlled magnetic anisotropy (VCMA) into the thin-film material system. By applying a vertical electric field via a dielectric gate, it controls the interface PMA strength, thereby achieving real-time adjustment of the free layer flipping behavior[55]. In 2014, Naik et al.[56] from the Data Storage Institute in Singapore achieved an electric-field-tunable magnetic sensor in CoFeB/MgO MTJs based on interface PMA. The sensor exhibited a sensitivity as high as 80.8 V cm^{-1} Oe^{-1} at room temperature, with sensitivity precisely controllable by the strength and polarity of the applied electric field. This method features low power consumption and fast response speed, making it suitable for constructing reconfigurable, adaptive magnetic sensors. Stress control integrates MTJs onto piezoelectric substrates. External voltage induces substrate strain, which modulates the magnetic anisotropy of the ferromagnetic layer, thereby achieving dynamic linear region offset and gain adjustment. In 2018, Ota et al.[57] from the University of Tokyo successfully achieved effective control of the magnetic anisotropy of cobalt layers by applying strain on flexible substrates. They constructed GMR devices capable of detecting strain direction, providing a new idea for achieving linear range control of TMR sensors through strain modulation. Although these methods offer new approaches for range control, issues such as high process complexity, poor real-time performance and reliability, and deteriorated noise levels remain to be further studied and improved.

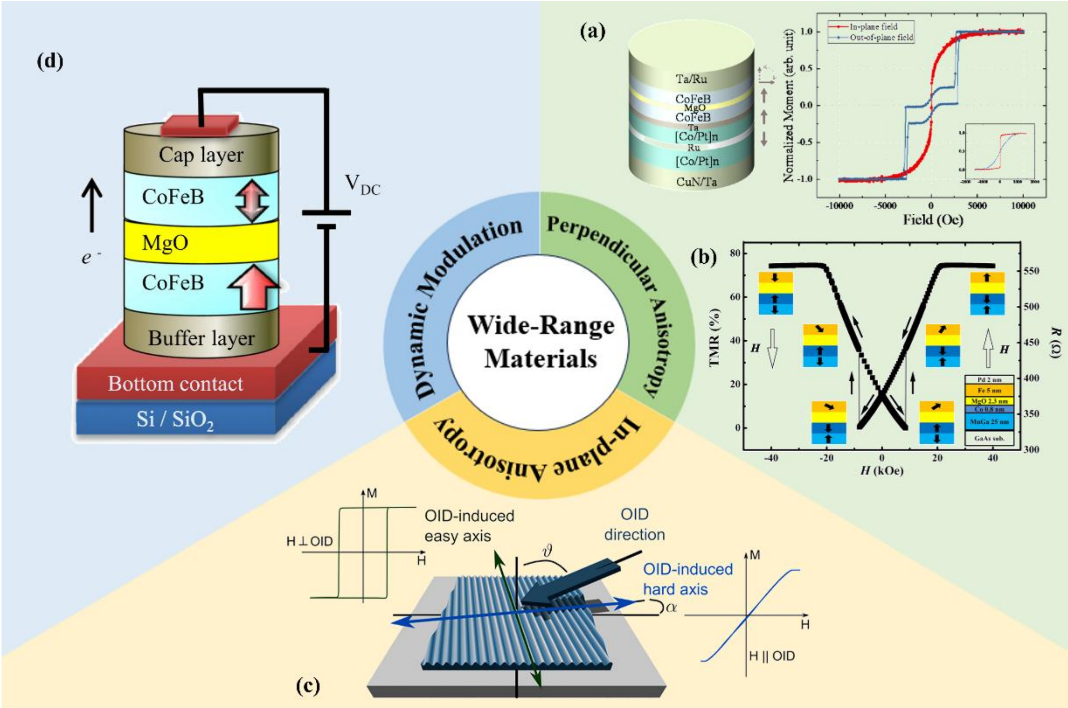

Fig. 4 Schematic diagram illustrating the development directions of wide-range thin-film material systems: (a) Interfacial-induced anisotropic PMA-MTJ and its in-plane/out-of-plane magnetoresistance response curves[58]; (b) Intrinsically crystal-anisotropic PMA-MTJ and its out-of-plane magnetoresistance response curve[48]; (c) Inclined sputtering deposition introduces in-plane uniaxial anisotropy to achieve range expansion[53]; (d) Electric-field-tunable dynamic-range TMR magnetic sensor[56].

3.3 Structural Optimization

The thin-film material system establishes the performance foundation of TMR sensors. Optimizing the sensitive structure is key to achieving performance breakthroughs. Synergistic innovations in MTJ structure, magnetic sensing element integration, and modulation techniques can further enhance sensitivity, broaden the linear range, and suppress noise.

3.3.1 MTJ Structure Optimization

Geometric design is a key method for controlling magnetic anisotropy and demagnetizing field distribution in the structural optimization of individual magnetic tunnel junctions (MTJs). Traditional rectangular MTJs introduce in-plane shape anisotropy by adjusting the aspect ratio. This guides the free layer magnetic moment to preferentially align along the long axis, thereby affecting the magnetoresistance ratio and sensitivity. However, sharp corners easily cause localized accumulation of magnetic charges. This forms strong local demagnetizing fields and induces non-uniform magnetization reversal processes. These processes are often accompanied by significant hysteresis and nonlinear response, limiting their application in high-precision sensing. To overcome these issues, smooth contour structures such as ellipses and rounded rectangles have been widely introduced. These designs optimize edge curvature to make surface magnetic charge distribution more uniform. This effectively alleviates the concentration of demagnetizing fields at corners and suppresses local magnetic domain nucleation and pinning. Consequently, the magnetization reversal process of the free layer becomes continuous and smooth. This significantly improves the linearity of the magnetic response and reduces hysteresis errors.

To further break through the bottlenecks in linear range and dynamic performance, the magnetic vortex state structure has been introduced into MTJs. When the lateral dimensions of the MTJ free layer exceed the material's exchange length and possess an appropriate aspect ratio, the system tends to form an energy-stable closed-flux structure, namely the magnetic vortex state, as shown in Figure 5(b). In this state, in-plane magnetic moments arrange in a rotating closed pattern around the central vortex core. This significantly reduces demagnetizing energy. The structure responds to external fields through the continuous displacement of the vortex core, rather than the overall reversal of magnetic moments seen in traditional MTJs. This mechanism avoids abrupt magnetization switching, achieving highly linear and nearly hysteresis-free output characteristics[59,60]. The team led by Xiao at Brown University in the United States[61] fabricated vortex-state MTJs that maintain a nonlinearity better than 0.5% within a magnetic field range of up to 100 Oe. The resolution reaches 18 $\mathrm{nT}/\sqrt{\mathrm{Hz}}$ at a frequency of 1 Hz. Furthermore, the closed magnetic flux characteristic within the structure effectively suppresses magnetic dipole coupling between units. This facilitates high-density array integration and low-crosstalk operation, providing an ideal structural basis for high-precision, wide-dynamic-range magnetic sensors. In 2025, the same team[17] expanded the diameter of the MTJ free layer to 40 μm to further optimize the sensitivity metrics of magnetic vortex-state MTJs. Test results indicated that the DC sensitivity of large-size vortex-state MTJs reached 2.80%/Oe. This represents an approximately eightfold improvement compared to traditional small-diameter vortex devices. The device maintained nearly hysteresis-free response characteristics throughout its linear operating range. This verified the feasibility of achieving ultra-high sensitivity while maintaining excellent linearity using large-diameter vortex states. Additionally, the magnetic vortex state exhibits excellent resistance to magnetic field shocks. Liu et al.[22] demonstrated that the output characteristics of vortex-state TMR sensors remained stable after multi-directional magnetic field shocks of ±1 kOe. The nonlinearity increased only from 0.3% to 0.5%. In contrast, traditional TMR sensors showed significant deterioration in hysteresis. This highlights the unique advantages of the magnetic vortex state structure in environments with strong electromagnetic interference.

On the other hand, magnetic yoke design further enhances device sensitivity and signal-to-noise ratio by introducing extended soft magnetic electrode layers to reconstruct the magnetization evolution path of the free layer, as shown in Figure 5(c). Magnetic yokes are typically composed of soft magnetic materials with high permeability and low coercivity. Their long arms guide magnetic flux concentration and homogenize the magnetization distribution within the free layer. This promotes coherent rotation of magnetic moments under external fields and suppresses disordered reversal and local pinning in edge regions. This controlled magnetization rotation mechanism significantly enhances the repeatability of the magnetic response while reducing low-frequency magnetic noise. Chen et al.[62] showed that MTJ sensors based on magnetic yoke structures achieve sensitivities exceeding 27%/mT. Moreover, their $1/f$ low-frequency noise level is nearly an order of magnitude lower than that of traditional structures. This demonstrates great potential for weak magnetic field detection scenarios, such as biomagnetic signal monitoring and microcurrent detection.

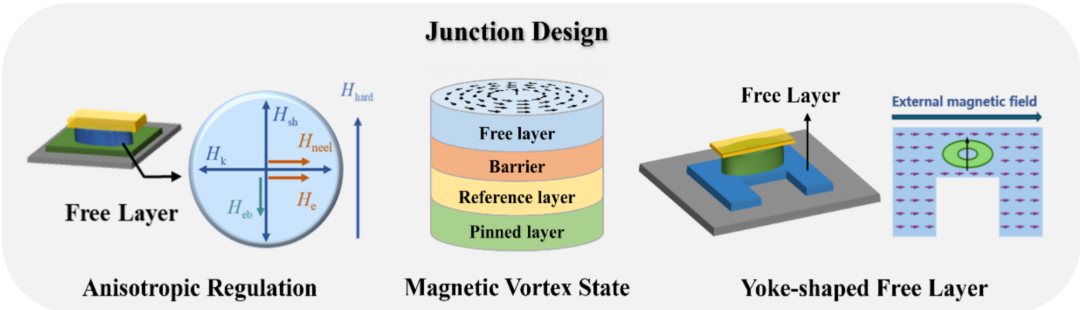

Fig. 5 Schematic diagram of MTJ structure optimization: (a) Anisotropy regulation (including geometric shape design and annealing process); (b) magnetic vortex state structure design; (c) magnetic yoke structure design.

In addition to the geometric optimizations described above, post-annealing techniques play a critical role in regulating the performance of individual magnetic tunnel junctions (MTJs). Specifically, the two-step annealing process is a key technology for achieving orthogonal alignment of the reference and free layer magnetic moments, thereby obtaining a linear magnetic response curve. By designing different blocking temperatures for the two antiferromagnetic pinning layers within a dual-pinned thin-film material system, the first high-temperature annealing step initializes the reference layer magnetic moment and promotes ordered crystallization at the CoFeB/MgO interface. This significantly enhances the tunneling magnetoresistance (TMR) ratio. Subsequently, during the second low-temperature annealing step, an external magnetic field is applied in a specific direction to selectively reorient the exchange bias direction of the free layer while keeping the reference layer direction unchanged. This ultimately achieves an initial orthogonal configuration of the two magnetic moments. Although traditional two-step orthogonal annealing can achieve magnetic moment orthogonality, it often results in residual bias fields in the free layer due to the Néel coupling effect, which exacerbates zero-field offset. To address this issue, Zhang et al.[63] from the National University of Defense Technology proposed a non-orthogonal annealing (NOA) method. By setting the cooling magnetic field direction of the second annealing step at a non-orthogonal angle relative to the initial easy axis, this method cleverly introduces an effective compensation field component opposite to the direction of the Néel coupling field. Experimental results indicate that MTJ devices subjected to 120° non-orthogonal annealing exhibit a zero-field offset reduced to less than 1 Oe. This performance is significantly superior to the typical values obtained under orthogonal annealing. Furthermore, the linear response range extends into the weak-field region, and the sensitivity near zero field more than doubles. Additionally, to further improve the symmetry and linearity of the magnetic response, Sun et al.[19] from Beihang University proposed and verified a three-step annealing process. This process adds a third medium-to-low temperature annealing step to the two-step method, performing fine adjustments under a small magnetic field or in a specific direction. This step precisely calibrates the magnetic anisotropy axis and exchange bias direction of the free layer. It effectively mitigates anisotropy distortions or residual stresses potentially introduced in the first two steps, further reducing hysteresis and nonlinear errors. Consequently, high-performance metrics were achieved, including a sensitivity of 1.57 $mV \cdot V^{-1} \cdot Oe^{-1}$ and a resolution of 29.3 $nT/\sqrt{Hz}$@10 Hz.

3.3.2 Optimization of Magnetic Sensing Element Structure

In the structural optimization of TMR magnetic sensing elements, the series-parallel integration of MTJs and the Wheatstone bridge configuration constitute the fundamental technical pathways for enhancing overall sensor performance, as shown in Figure 6(a). Connecting multiple MTJ units in series or parallel not only effectively distributes the operating voltage but also reduces the risk of electrostatic breakdown in individual junctions caused by local electric field concentration. This improves device reliability and lifespan. Moreover, the statistical averaging effect derived from multi-junction integration significantly suppresses low-frequency 1/*f* noise. Research by Fujiwara et al.[11] at Tohoku University in Japan demonstrates that the total noise level decreases as the number of series-connected MTJ units increases. By connecting 100×100 MTJs in series, the team reduced the noise level to approximately 1/30 of that of a single junction, thereby substantially improving the signal-to-noise ratio and magnetic field detection resolution. Furthermore, constructing MTJ units into a Wheatstone bridge structure is a common method for achieving high sensitivity, low noise, and suppression of temperature drift. In traditional designs, the bridge typically consists of four MTJs with matched characteristics and high consistency. Differential output cancels common-mode interference, enhancing response sensitivity to magnetic field changes. However, fabricating four completely identical MTJ units presents significant process challenges. Mismatch between bridge arms leads to zero-field offset and non-ideal linear output, affecting sensor precision and stability. Therefore, future research must further explore on-chip bridge formation methods, such as local annealing and zoned lithography, to improve the consistency of bridge devices.

Magnetic flux concentrators (MFCs) are a primary means of enhancing TMR magnetic sensor sensitivity at the structural level. As shown in Figure 6(b), MFCs amplify weak magnetic fields to be measured and shield against interfering magnetic fields from other directions, thereby significantly improving the sensor's signal-to-noise ratio and sensitivity. Optimizing traditional MFCs requires collaborative design across multiple dimensions, including materials, gaps, shapes, and fabrication processes, to achieve optimal magnetic field enhancement. Regarding material selection, NiFe alloys[64] with high magnetic permeability and low magnetostriction coefficients are typically used. Electrochemical deposition technology enables reproducible, large-area formation at the wafer level. This ensures excellent soft magnetic properties and low coercivity, thereby reducing nonlinear response and hysteresis losses. Gap design is a critical factor in MFC optimization; narrow air gaps significantly enhance the local magnetic field concentration effect, increasing the magnetic field strength in the region of the MTJ junction. Manceau et al.[65] demonstrated that controlling the air gap between the MFC and the TMR sensor to 5-7 μm achieves a magnetic field gain of up to 440 times. Theoretically, this could increase TMR sensor sensitivity from 3.6%/mT to 1580%/mT. However, such narrow gaps impose extremely high requirements on manufacturing processes. Precise control of the TMR sensor's position within the gap is necessary to avoid asymmetry in magnetic field distribution caused by displacement, which would otherwise affect sensor linearity and sensitivity consistency. Regarding geometric configuration, optimization efforts have primarily focused on systematically studying the impact of different shapes and their dimensional ratios on magnetic gain and linear operating range through finite element simulation and experimental verification[66,67]. Bi et al.[68] from Tsinghua University systematically investigated the impact of geometric configurations such as trapezoidal, triangular, wedge-shaped, and horn-shaped MFCs on performance. They found that wedge-shaped MFCs provide the highest magnetic circuit gain, which is determined solely by the ratio of geometric parameters rather than their absolute values. However, the introduction of MFCs also brings new challenges, primarily additional magnetic noise and hysteresis. These issues mainly stem from residual mechanical stress generated during thin-film deposition, which may cause unstable magnetization reversal in the free layer or introduce low-frequency noise. Precisely regulating current density during electrochemical deposition can optimize the composition ratio and internal stress state of the NiFe alloy, thereby effectively suppressing hysteresis. Nevertheless, magnetic noise induced by the MFC itself in the low-frequency band remains difficult to eliminate completely. This must be comprehensively considered in subsequent signal conditioning circuits and system-level noise suppression strategies.

To further break the gain limits of single-layer MFCs, double-layer and even multi-layer magnetic flux concentrator structures have been proposed and are gradually being studied. These designs construct multi-stage magnetic circuits through nesting or cascading, achieving more efficient magnetic field compression and step-by-step amplification under the same external magnetic field excitation. In 2018, He et al.[69] adopted a double-layer MFC structure and finely matched the geometric parameters and gap coupling relationships between layers. Without significantly increasing the device area, they achieved a higher local field enhancement effect compared to single-layer MFC structures. The total MFC gain reached 516.9 times, enabling the MTJ sensor to achieve a sensitivity of 775.4%/Oe and a detection limit of 30 $\mathrm{pT}/\sqrt{\mathrm{Hz}}$@1 kHz.

Superconducting MFCs represent the frontier of magnetic field amplification technology. Their ultra-high amplification factor and extremely low magnetic field detection capability offer unique advantages in ultra-high sensitivity detection fields. A superconducting MFC consists of a closed loop made of superconducting film, containing a narrow section. When an external magnetic field passes vertically through the superconducting loop, shielding currents are generated due to the Meissner effect. The current density significantly increases in the narrow region, thereby forming a localized magnetic field enhancement[70-72]. In 2022, Yang et al.[73] from the National University of Defense Technology used a superconducting MFC with a 5 μm wide constriction region under a superconducting state at 77 K, achieving a maximum magnetic field amplification factor of 262 times. Theoretical calculations indicate that when the distance between the TMR and the superconducting MFC is reduced to within 0.5 μm, the magnetic field amplification factor can approach 1000 times. However, superconducting MFCs require operation in low-temperature environments, which limits their application in conventional scenarios. Furthermore, the need for refrigeration equipment prevents chip-scale integration, posing severe challenges for portable and low-cost magnetic sensor applications. Despite this, superconducting MFCs retain significant application value in fields requiring extremely high sensitivity, such as biomedical imaging and geophysical exploration.

3.3.3 Noise Modulation Techniques

The 1/*f* noise of TMR sensors is particularly significant in the low-frequency band, severely limiting their ability to detect weak magnetic fields. To overcome this problem, noise modulation techniques are widely adopted, as shown in Figure 6(c). The core idea is to modulate the low-frequency magnetic field signal to be measured into the high-frequency region via external driving. This avoids the frequency band dominated by 1/*f* noise. The signal is then demodulated to restore the original information, effectively improving the signal-to-noise ratio[74]. In 2002, Edelstein and Fischer[75] first proposed a concept for a torsional magnetic flux concentrator based on micro-electro-mechanical systems (MEMS). Electrostatic driving causes periodic rotation around the torsion arm axis, modulating the magnetic field in the sensitive area of the magnetic sensor to a high-frequency band at 29 kHz. This preliminary verified the feasibility of the technology. In 2008, Guedes et al.[76] from the INESC-MN Institute in Portugal used an electrostatically driven cantilever structure to drive the magnetic flux concentrator into resonance. They increased the magnetic field modulation frequency at the GMR spin valve to 460 kHz, achieving a modulation efficiency of 0.11%. Subsequently, through structural optimization using micro-torsion actuators instead of cantilevers, they improved the modulation efficiency to 11%[77]. However, such MEMS modulation systems based on electrostatic driving have complex structures, are difficult to fabricate, and still require improved modulation efficiency.

Regarding the optimization of magnetic flux modulation structures, vertical motion flux modulation (VMFM) and magnetic flux electric modulation (MFEM) are two representative technical pathways. VMFM is a mechanical modulation method based on MEMS. In 2012, Hu et al.[78] from the National University of Defense Technology proposed a VMFM structure based on a piezoelectric-driven cantilever. Experiments showed that its field modulation efficiency reached 18.8%, and the noise level decreased to approximately $0.44\,\mathrm{nT}/\sqrt{\mathrm{Hz}}$. This method uses a piezoelectric-driven cantilever structure to drive a flux modulation film (FMF) to vibrate periodically in the vertical direction. This modulates the magnetic flux by changing the magnetic flux path. When the flux modulation film approaches the air gap, magnetic flux preferentially passes through this high-permeability film, causing the magnetic field in the gap to weaken. When the FMF moves away, the magnetic field in the gap recovers. This periodic change converts the low-frequency magnetic field to be measured into a high-frequency AC signal, thereby suppressing 1/*f* noise. To further improve performance, Du et al.[79] proposed a piezoelectric-driven double-clamped beam modulation structure with amplitude feedback in 2019. By optimizing the initial height of the modulation film, vibration amplitude, and material properties, they significantly increased the modulation efficiency to 68.7% and improved detection capability by approximately 43 times. Nevertheless, VMFM technology still relies on mechanical vibration. It suffers from issues such as high driving voltage, high power consumption, and modulation frequency limitations imposed by mechanical resonance. Furthermore, mechanical vibration may cause structural instability and output drift, affecting the long-term reliability of the sensor.

To overcome the limitations of mechanical modulation, Pan et al.[80] proposed an MFEM method based on a FeSiBPC/PMN-PT multiferroic heterostructure, achieving a magnetic susceptibility regulation capability of up to 150 times. Under conditions of a 10 V driving voltage and a 50 μm thick ferroelectric layer, the theoretical modulation efficiency can reach 73%. This method utilizes the magnetoelectric coupling effect of ferroelectric/ferromagnetic (FE/FM) multiferroic heterostructures to achieve non-mechanical modulation of magnetic permeability via voltage control. Specifically, in the FE/FM heterostructure, the ferroelectric layer generates anisotropic strain under external voltage. This strain is transmitted to the ferromagnetic layer through the interface, thereby adjusting the magnetic permeability of the ferromagnetic layer through the magnetostriction effect. This achieves effective regulation of magnetic flux. The advantage of this method lies in the absence of mechanical motion. The modulation frequency can theoretically reach hundreds of megahertz, far exceeding the limits of mechanical resonance frequencies. Additionally, by avoiding mechanical vibration, the system structure is more stable, power consumption is lower, and it is easier to compatible with integrated circuit processes. This provides a new pathway for high-frequency, high-precision magnetic sensing[81].

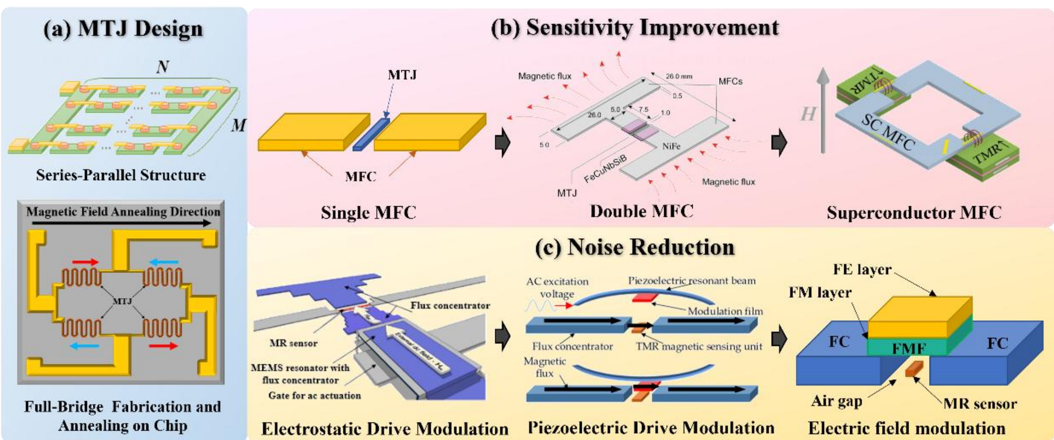

Fig. 6 Schematic diagram of the optimization of magnetosensitive body structures: (a) Series-parallel design and on-chip integrated annealing; (b) Sensitivity enhancement methods: single-layer flux concentrators, double-layer flux concentrators[82], and superconducting flux

concentrators; (c) Noise suppression methods: electrostatic drive modulation[83], piezoelectric drive modulation[84], and electric field modulation.

4 Application Scenarios

TMR magnetic sensors offer core advantages, including high sensitivity, high-frequency response, low power consumption, compact size, and compatibility with CMOS processes. Consequently, they demonstrate broad application prospects in frontier fields such as biomedical engineering and smart grids.

4.1 Biomedical Applications

Biomagnetic signals, such as magnetocardiography (MCG) and magnetoencephalography (MEG), propagate without attenuation through human tissue. These signals offer high fidelity, high spatial resolution, and non-contact measurement capabilities, making them essential for non-invasive physiological monitoring. Currently, superconducting quantum interference devices (SQUIDs) are the mainstream equipment for biomagnetic detection. However, SQUIDs require liquid helium cooling, resulting in bulky systems, high costs, and limited portability. As a high-sensitivity magnetic sensing technology operable at room temperature, TMR sensors have achieved magnetic field detection capabilities in the sub-picotesla (sub-pT) range[42]. This advancement provides key technical support for developing low-cost, miniaturized, and deployable biomagnetic measurement systems. In recent years, significant breakthroughs in material and device structure designs have enhanced TMR sensor sensitivity to $0.94\ \mathrm{pT}/\sqrt{\mathrm{Hz}}@1\ \mathrm{Hz}$. This performance approaches that of SQUIDs while maintaining advantages such as room-temperature operation, low power consumption, and high integration. Regarding practical applications, Fujiwara et al.[41] first measured MCG signals using optimized TMR sensors in a magnetically shielded room in 2018. They successfully captured the R-wave in the MCG and clearly presented the QRS complex through signal averaging, verifying the feasibility of TMR technology for room-temperature biomagnetic detection. In 2021, Oogane et al.[42] optimized TMR sensor performance to clearly observe the MCG QRS complex without signal averaging. This achievement demonstrates significant potential for real-time, dynamic magnetocardiographic monitoring. In 2023, Kurashima et al.[85] developed a high-precision TMR magnetocardiography system that operates without a magnetically shielded room. This system integrates 288 TMR sensors into an arch-shaped array. By combining dual-stage flux concentrators, a closed-loop feedback mechanism, and signal spatial separation algorithms, it achieved a magnetic field resolution of $0.99\ \mathrm{pT}/\sqrt{\mathrm{Hz}}$ in normal working environments. The system obtained high-quality magnetocardiograms comparable to those from SQUIDs, marking a critical step toward the clinical practicality of TMR technology.

Furthermore, the industry is actively promoting the practical application of TMR biomagnetic detection systems. In 2016, TDK Corporation of Japan collaborated with Tokyo Medical and Dental University to launch an MCG detection system based on TMR sensor arrays. This system achieved the world's first measurement and imaging visualization of magnetic heart fields. With a magnetic field resolution reaching tens of pT, it holds promise for early screening of heart disease and fetal magnetocardiographic monitoring. In 2023, the UK startup Neuranics launched a wearable MCG development platform. This platform detects weak magnetic signals at the pT level and transmits cardiac magnetic signals in real time to smart devices such as mobile phones and tablets via Bluetooth. This enables 24 h all-weather cardiac health monitoring. Domestic enterprises, such as MultiDimension Technology, launched a new compact, high-precision, low-noise linear TMR magnetic sensor with a 3 pT level in 2024. In collaboration with the research team at Ningbo University, they completed joint testing of TMR sensor MCG signal detection. The measured MCG waveforms clearly distinguished the P, Q, R, S, T, and U waves. These commercial advancements indicate that TMR technology is accelerating its transition from laboratories to clinical applications. This shift promotes the transformation of biomagnetic detection toward low-cost and wearable solutions. With superior detection performance, comprehensive system integration, and algorithmic support, TMR technology is poised to extend biomagnetic detection from large-scale equipment to wearable scenarios. This evolution will reshape the technological landscape of physiological functional imaging and health monitoring[4,86-88].

4.2 Smart Grids

With the large-scale integration of renewable energy and the advancement of "dual carbon" goals, smart grids impose higher requirements on the accuracy, bandwidth, reliability, and real-time performance of current monitoring. Due to their high sensitivity, wide frequency response, low power consumption, wide dynamic range, and good temperature stability, TMR sensors have become ideal non-contact current sensing solutions for smart grid construction[74,89]. In practical applications, TMR-based current sensing technology has achieved several key breakthroughs. Lu Wenshuai et al.[90] developed a non-invasive current monitoring microsystem without a magnetic core structure using a monolithic single-axis TMR sensor design. Within a measurement range of 0—8 A, the maximum relative error was only 1.5%, meeting the national standard for 0.5-level accuracy. Regarding bandwidth expansion, Ziegler et al.[91] proposed a hybrid wideband current sensor that combines the advantages of TMR sensors and Rogowski coils. With an ultra-wide bandwidth from DC to 315 MHz, this sensor was successfully applied to measure commutation currents in fast-switching power electronics. In terms of anti-interference, Liu et al.[92] proposed a TMR current sensing scheme based on a dual-circular PCB trace structure. This approach uses a differential structure to convert external interference into common-mode signals, significantly enhancing anti-interference capability. Experiments demonstrated that this method maintains a sensitivity of 0.5902 V/A even with a 2 mm installation error, exhibiting strong robustness against sensor installation deviations.

In the commercial sector, several sensor companies, including Allegro, TDK, Sinomags Technology, and MultiDimension Technology, have deployed TMR current sensors. In 2025, Allegro's XtremeSense brand launched the industry's first mass-produced magnetic current sensor with a 10 MHz bandwidth. This sensor features a response time as low as 50 ns and a measurement noise of only 26 mA RMS across the full 10 MHz bandwidth. It offers a novel solution for high-voltage power conversion, particularly in wide-bandgap applications. In the same year, the domestic company Sinomags Technology also released a MHz-level high-frequency current sensor. This device achieves a response speed of 200 ns and covers a wide range of 100—1000 A with a high precision of ±1%, representing an industry-leading level. Additionally, companies such as TDK and MultiDimension Technology have introduced mature product series. Their performance in bandwidth, range, and linearity meets the usage requirements of various scenarios in the smart grid field. These products strongly support improvements in the real-time performance and reliability of smart grid state perception. In the future, TMR current sensors will become indispensable key components in the intelligent construction of power systems.

4.3 Other Applications

Beyond biomedical applications and smart grids, TMR sensors are accelerating their penetration into consumer electronics, industrial automation, and automotive electronics markets, gradually replacing traditional Hall and other magnetoresistive (MR) sensors. In consumer electronics, electronic compasses in smartphones represent a significant application of TMR sensors. Compared to anisotropic magnetoresistance (AMR) solutions, TMR electronic compasses offer lower power consumption and higher angular resolution, enhancing user experiences in navigation and augmented reality. Furthermore, TMR linear sensors are widely used in magnetic axis keyboards for laptops, optical image stabilization (OIS) position detection for smartphone cameras, and trigger key detection for high-end game controllers due to their high sensitivity, precision, and reliability. In industrial automation, TMR sensors provide critical position and angle feedback for industrial robots and precision motor control.

For instance, TMR angle sensors at robot joints enable absolute position measurement, offering strong anti-interference capabilities and long service life. In high-speed, high-precision servo motor control, TMR-based alternatives to resolvers provide finer resolution and faster dynamic response. In automotive electronics, TMR applications have expanded beyond early wheel speed sensing to more core areas. In addition to resolvers for motor control, TMR current sensors are widely used in battery management systems and motor drive units. They precisely monitor charging/discharging currents and phase currents, with their wide range and high bandwidth characteristics perfectly matching the needs of electric vehicles. Moreover, TMR sensors for gearbox gear detection and steering wheel angle measurement are favored for their stability across wide temperature ranges. Mainstream automotive chip suppliers, such as NXP, Infineon, and Allegro, have incorporated TMR sensing technology into their product roadmaps, demonstrating the vast application prospects of this technology.

5 Summary and Future Outlook

TMR sensors demonstrate significant application prospects in modern sensing technology due to their high sensitivity, low power consumption, miniaturization, wide frequency response, and good integrability. From position and current detection in industrial automation to MCG and neural signal monitoring in biomedicine, and further to drone navigation, geological exploration, and environmental perception in IoT terminals, TMR sensors are gradually replacing traditional Hall, AMR, and giant magnetoresistance (GMR) devices. They are becoming the preferred solution for high-precision magnetic field detection. The physical mechanism based on the quantum tunneling effect endows these devices with a signal-to-noise ratio and resolution far exceeding other magnetoresistive technologies. Particularly in weak magnetic field detection, they exhibit performance potential approaching that of SQUIDs, while not requiring low-temperature operating environments. This offers greater practicality and deployment flexibility. With the rapid development of artificial intelligence, wearable devices, and edge computing, TMR sensors are not only serving as front-end sensing units but are also gradually integrating into intelligent sensing systems. This integration is driving a paradigm shift in next-generation magnetic sensing technology.

The current technological development path of TMR sensors proceeds in parallel along three directions: material optimization, structural innovation, and system integration. Looking ahead, the development of TMR sensors still faces several key challenges and breakthrough directions.

First, regarding material system optimization, developing TMR thin-film material systems with higher sensitivity and wider dynamic ranges is a primary future direction. On one hand, to meet higher-precision detection needs such as biomagnetic sensing, it is urgent to further improve the magnetoresistance ratio and sensitivity of devices. This can be achieved by developing new barrier layer materials and composite free layers, thereby reducing intrinsic noise and achieving higher magnetic field detection resolution to suit application requirements. On the other hand, scenarios such as automotive electronics and smart grids require TMR sensors to have a linear measurement dynamic range reaching the thousand-Oersted (Oe) level[6,93]. This necessitates precise control of the magnetic anisotropy of the free layer to balance sensitivity and range, avoiding saturation distortion under strong fields. Meanwhile, enhancing thermal stability is a crucial aspect of material system optimization. To meet the stringent reliability requirements of automotive, industrial, and aerospace fields, it is necessary to maintain the stability of magnetic sensitivity characteristics over a wide temperature range. This can be achieved through interface engineering, barrier layer optimization, and the design of magnetic coupling systems, preventing performance degradation or parameter drift due to temperature fluctuations. Additionally, given the broad prospects of biomedical wearable electronics and flexible robotics, there is an urgent need to develop high-performance flexible TMR sensors. Achieving this goal requires high-quality growth of TMR films on flexible substrates. It also requires ensuring that devices maintain stable and reliable magnetic sensitivity under mechanical stresses such as repeated bending and stretching, posing extremely high demands on materials and fabrication processes.

Second, achieving high-performance, miniaturized three-axis TMR magnetic vector sensing is a current technical bottleneck. Three-axis sensors can completely capture magnetic field vector information, which is crucial for applications such as attitude determination and navigation positioning[94-97]. However, existing mainstream integration schemes have obvious defects. Assembly-type three-axis schemes orthogonally mount three single-axis chips, resulting in large volumes and difficulty in ensuring orthogonal accuracy. Magnetic flux-guiding schemes use soft magnetic materials to guide the magnetic field. Although they achieve monolithic integration, they introduce nonlinearity, hysteresis, and additional noise, and require substantial computation for decoupling magnetic fields in different directions. Sloped-substrate schemes fabricate sensors on inclined substrates, which involves complex processes and poor consistency across different directions. Therefore, future research needs to further explore monolithic miniaturized three-axis TMR magnetic sensing technologies based on the fusion of multi-physics effects, such as the anomalous Hall effect, magnetoelectric coupling materials, and two-dimensional van der Waals materials. This approach aims to fundamentally resolve the inherent contradictions among orthogonal accuracy, packaging volume, and CMOS process compatibility in three-axis sensors.

Finally, exploring the frontier integration of TMR sensors with artificial intelligence is key to unlocking their future development potential. The magnetic tunnel junctions (MTJs) in TMR sensors possess characteristics such as non-volatility and multiple resistance states[98-101], demonstrating the potential for "sensing-memory-computing integration." However, integrating these physical properties into sensor design to develop dedicated "sensing-memory-computing integrated" architectures remains a current development challenge. On one hand, at the algorithmic level, deep learning can be used to process complex magnetic signals collected by TMR sensor arrays. This enables pattern recognition, noise suppression, and target classification, greatly enhancing the perceptual intelligence of the system. A more revolutionary direction lies at the hardware level, where the analog resistive switching behavior of TMR junctions is directly used to construct artificial synapses and neurons. This allows certain computational tasks, such as spiking neural network processing, to be completed in situ at the sensing end. This approach not only achieves ultra-low power consumption and ultra-high parallelism in data processing but also constructs a true sensing-memory-computing integrated system. It provides a novel solution for edge intelligence and real-time processing in specific scenarios.

In summary, TMR sensors are at a critical stage of evolving from single-function devices to multifunctional, intelligent, and systematic sensing platforms. Although challenges remain in material innovation, three-dimensional integration, flexibility, and intelligent algorithm fusion, continuous breakthroughs in interdisciplinary technologies are expected. TMR sensors are poised to play a more core role in next-generation intelligent sensing systems. This will promote their extensive application and deep penetration in frontier fields such as healthcare, autonomous driving, industrial IoT, and space exploration.

References

[1] Zheng C, Zhu K, Cardoso De Freitas S, Chang J Y, Davies J E, Eames P, Freitas P P, Kazakova O, Kim C, Leung C W, Liou S H, Ognev A, Piramanayagam S N, Ripka P, Samardak A, Shin K H, Tong S Y, Tung M J, Wang S X, Xue S, Yin X, Pong P W T 2019 *IEEE Trans. Magn.* **55** 1

[2] Yang S, Zhang J 2021 *Chemosensors* **9** 211

[3] Julliere M 1975 *Phys. Lett. A* **54** 225

[4] Oogane M 2024 *IEICE Trans. Electron. E* **107.C** 171

[5] Yan S H, Zhou Z T, Yang Y D, Leng Q W, Zhao W S 2022 *Tsinghua Sci. Technol.* **27** 443

[6] Leitao D C, Riel F J F V, Rasly M, Araujo P D R, Salvador M, Paz E, Koopmans B 2024 *Npj Spintronics* **2** 54

[7] Malinowski G, Hehn M, Sajieddine M, Montaigne F, Jouguelet E, Canet F, Alnot M, Lacour D, Schuhl A 2003 *Appl. Phys. Lett.* **83** 4372

[8] Negulescu B, Lacour D, Montaigne F, Gerken A, Paul J, Spetter V, Marien J, Duret C, Hehn M 2009 *Appl. Phys. Lett.* **95** 112502

[9] Djayaprawira D D, Tsunekawa K, Nagai M, Maehara H, Yamagata S, Watanabe N, Yuasa S, Suzuki Y, Ando K 2005 *Appl. Phys. Lett.* **86** 092502

[10] Chen J Y, Feng J F, Coey J M D 2012 *Appl. Phys. Lett.* **100** 142407

[11] Fujiwara K, Oogane M, Nishikawa T, Naganuma H, Ando Y 2013 *Jpn. J. Appl. Phys.* **52** 04CM07

[12] Han X F, Zhang Y, Feng J F, Chen C, Deng H, Huang H, Guo J H, Liang Y, Si W R, Jiang A F, Wei H X 2022 *Acta Phys. Sin.* **71** 238502

[13] Zhao W S, Zhang B Y, Peng S Z 2023 *Spintronic Science and Technology* （Beijing: Posts & Telecom Press） pp320–324

[14] Zhong Z Y 2015 *Magnetoresistive Sensors* （Beijing: Science Press） pp32–33

[15] Ye X B 2022 *Sensors and Detection Technology*（Beijing: China Machine Press） pp84–86

[16] Nakano T, Fujiwara K, Oogane M 2025 *Appl. Phys. Lett.* **126** 160503

[17] Brown B J, Mitchell L K, Bheemarasetty V S, Cao H M, Kingsnorth J N, Sanes J N, Xiao G 2025 *Phys. Rev. Appl.* **24** 034063

[18] Cardoso S, Leitao D C, Gameiro L, Cardoso F, Ferreira R, Paz E, Freitas P P 2014 *Microsyst. Technol.* **20** 793

[19] Sun Y, Xia Q, Zhang D, Mou Q, Li Y, Xie L, Guang S, Cao Z, Zhu D, Zhao W 2024 *AIP Adv.* **14** 015304

[20] Luo J, Xu Z, Jin Z, Wang M, Cai X, Chen J 2024 *ACS Appl. Mater. Interfaces* **16** 31677

[21] Han X F, Zhang Y, Wang Y Z, Huang L, Ma Q L, Liu H F, Wan C H, Feng J F, Yin L, Yu G Q, Yu T, Yan Y 2021 *Chin. Phys. Lett.* **38** 128501

[22] Liu J, Guan M, Gong Y, Ni F, Gao X, Su W, Wang Z, Jiang Z, Hu Z, Liu M 2024 *IEEE Electron Device Lett.* **45** 1289

[23] Yao X P, Pan M C, Ji M H, Hu J F, Zhang Q, Li P S 2023 *Transducer Microsyst. Technol.* **42** 21

[24] Miyazaki T, Tezuka N 1995 *J. Magn. Magn. Mater.* **139** 231

[25] Moodera J S, Kinder L R, Wong T M, Meservey R 1995 *Phys. Rev. Lett.* **74** 3273

[26] Butler W H, Zhang X G, Schulthess T C, MacLaren J M 2001 *Phys. Rev. B* **63** 054416

[27] Yuasa S, Nagahama T, Fukushima A, Suzuki Y, Ando K 2004 *Nat. Mater.* **3** 868

[28] Parkin S S P, Kaiser C, Panchula A, Rice P M, Hughes B, Samant M, Yang S H 2004 *Nat. Mater.* **3** 862

[29] Ikeda S, Hayakawa J, Ashizawa Y, Lee Y M, Miura K, Hasegawa H, Tsunoda M, Matsukura F, Ohno H 2008 *Appl. Phys. Lett.* **93** 082508

[30] Scheike T, Wen Z, Sukegawa H, Mitani S 2023 *Appl. Phys. Lett.* **122** 112404

[31] Das Sarma S, Adam S, Hwang E H, Rossi E 2011 *Rev. Mod. Phys.* **83** 407

[32] Karpan V M, Khomyakov P A, Starikov A A, Giovannetti G, Zwierzycki M, Talanana M, Brocks G, van Den Brink J, Kelly P J 2008 *Phys. Rev. B* **78** 195419

[33] Pan M C, Li P, Qiu W, Zhao J, Peng J, Hu J, Hu J, Tian W, Hu Y, Chen D, Wu X, Xu Z, Yuan X 2018 *J. Magn. Magn. Mater.* **453** 101

[34] Thapa A, Sharma B 2025 *Adv Mater. Technol.* **10** e00133

[35] Mi M, Xiao H, Yu L, Zhang Y, Wang Y, Cao Q, Wang Y 2023 *Materials Today Nano* **24** 100408

[36] Fujiwara K, Oogane M, Yokota S, Nishikawa T, Naganuma H, Ando Y 2012 *J. Appl. Phys.* **111** 07C710

[37] Liu F, Zhou H, Yuan L, Cai Y 2023 *BMC Nurs* **22** 483

[38] Yuan Z H, Huang L, Feng J F, Wen Z C, Li D L, Han X F, Nakano T, Yu T, Naganuma H 2015 *J. Appl. Phys.* **118** 053904

[39] Yuan Z H, Feng J F, Guo P, Wan C H, Wei H X, Ali S S, Han X F, Nakano T, Naganuma H, Ando Y 2016 *J. Magn. Magn. Mater.* **398** 215

[40] Huang L, Yuan Z H, Tao B S, Wan C H, Guo P, Zhang Q T, Yin L, Feng J F, Nakano T, Naganuma H, Liu H F, Yan Y, Han X F 2017 *J. Appl. Phys.* **122** 113903

[41] Fujiwara K, Oogane M, Kanno A, Imada M, Jono J, Terauchi T, Okuno T, Aritomi Y, Morikawa M, Tsuchida M, Nakasato N, Ando Y 2018 *Appl. Phys. Express* **11** 023001

[42] Oogane M, Fujiwara K, Kanno A, Nakano T, Wagatsuma H, Arimoto T, Mizukami S, Kumagai S, Matsuzaki H, Nakasato N, Ando Y 2021 *Appl. Phys. Express* **14** 123002

[43] Matos F, Macedo R, Freitas P P, Cardoso S 2023 *AIP Adv.* **13** 025108

[44] Akamatsu S, Oogane M, Tsunoda M, Ando Y 2020 *AIP Adv.* **10** 015302

[45] Akamatsu S, Oogane M, Tsunoda M, Ando Y 2022 *AIP Adv.* **12** 075021

[46] Roy T, Tsujikawa M, Kanemura T, Shirai M 2020 *J. Magn. Magn. Mater.* **498** 166092

[47] Tsuchiya T, Roy T, Elphick K, Okabayashi J, Bainsla L, Ichinose T, Suzuki K Z, Tsujikawa M, Shirai M, Hirohata A, Mizukami S 2019 *Phys. Rev. Mater.* **3** 084403

[48] Zhao X P, Lu J, Mao S W, Yu Z F, Wang H L, Wang X L, Wei D H, Zhao J H 2017 *J. Phys. D: Appl. Phys.* **50** 285002

[49] Zeng Z M, Khalili Amiri P, Katine J A, Langer J, Wang K L, Jiang H W 2012 *Appl. Phys. Lett.* **101** 062412

[50] Nakano T, Oogane M, Naganuma H, Ando Y 2015 *IEEE Trans. Magn.* **51** 1

[51] Nakano T, Oogane M, Furuichi T, Ando Y 2017 *Appl. Phys. Lett.* **110** 012401

[52] Santos P, Araujo P, Sørensen D, Matos F, Freitas P P, Cardoso S 2023 *IEEE Trans. Magn.* **59** 1

[53] Willing S, Schlage K, Bocklage L, Ramin Moayed M M, Gurieva T, Meier G, Röhlsberger R 2021 *ACS Appl. Mater. Interfaces* **13** 32343

[54] Teixeira B M S, Timopheev A A, Caçoilo N, Cuchet L, Mondaud J, Childress J R, Magalhães S, Alves E, Sobolev N A 2020 *J. Phys. D: Appl. Phys.* **53** 455003

[55] Shao Y, Khalili Amiri P 2023 *Adv Mater. Technol.* **8** 2300676

[56] Naik V B, Meng H, Liu R S, Luo P, Yap S, Han G C 2014 *Appl. Phys. Lett.* **104** 232401

[57] Ota S, Ando A, Chiba D 2018 *Nat. Electron.* **1** 124

[58] Yan S H, Zhou Z T, Cao Z Q, Yang Y D, Li Z, Chen W B, Leng Q W, Zhao W S 2021 *2021 5th IEEE Electron Devices Technology & Manufacturing Conference*（*EDTM*） Chengdu, China, April 8–11, 2021 p1

[59] Suess D, Bachleitner-Hofmann A, Satz A, Weitensfelder H, Vogler C, Bruckner F, Abert C, Prügl K, Zimmer J, Huber C, Luber S, Raberg W, Schrefl T, Brückl H 2018 *Nat. Electron.* **1** 362

[60] Weitensfelder H, Brueckl H, Satz A, Pruegl K, Zimmer J, Luber S, Raberg W, Abert C, Bruckner F, Bachleitner-Hofmann A, Windl R, Suess D 2018 *Phys. Rev. Appl.* **10** 054056

[61] He G, Zhang Y, Xiao G 2020 *Phys. Rev. Appl.* **14** 034051

[62] Chen J Y, Carroll N, Feng J F, Coey J M D 2012 *Appl. Phys. Lett.* **101** 262402

[63] Zhang X, Pan M, Lei S, Ji M, Hu Y, Hu J, Chen D, Peng J, Qiu W, Li P 2024 *Appl. Phys. Lett.* **124** 052404

[64] Choi J G, Hwang D G, Rhee J R, Lee S S 2010 *J. Magn. Magn. Mater.* **322** 2191

[65] Manceau S, Brun T, Fischer J, Ducruet C, Sabon P, Cavoit C, Jannet G, Pinçon J L, Prejbeanu I L, Kretzschmar M, Baraduc C 2023 *Appl. Phys. Let.* **123** 082405

[66] Zhang X, Bi Y, Chen G, Liu J, Li J, Feng K, Lv C, Wang W 2018 *AIP Adv.* **8** 125222

[67] Feng Y, Chen J Y, Wu K, Wang J P 2020 *J. Magn. Magn. Mater.* **511** 166728
[68] Bi R, Zhang H, Pan S, Liu X, Chen R, Wu S, Hu J 2025 *Sensors* **25** 4739
[69] He G, Zhang Y, Qian L, Xiao G, Zhang Q, Santamarina J C, Patzek T W, Zhang X 2018 *Appl. Phys. Lett.* **113** 242401
[70] Wu Y, Xiao L, Hou S, Gao Z, Han L 2019 *IEEE Trans. Appl. Supercond.* **29** 1
[71] Han S, Wu Y, Wang Y, Chen J 2024 *Cryogenics* **138** 103803
[72] Wu Y, Xiao L Y, Hou S Z 2019 *Physics* **48** 14
[73] Yang L, Sun K, Tao J, Zhang X, Huang D, Pan M, Hu J, Qiu W, Ji M, Hu Y, Li P, Chen D, Zhang Q, Peng J 2022 *Sens. Actuators, A* **342** 113658
[74] Jiao Q, Jin Z, Zhang C, Chen J 2025 *Measurement* **242** 116143
[75] Edelstein A S, Fischer G A 2002 *J. Appl. Phys.* **91** 7795
[76] Guedes A, Patil S B, Cardoso S, Chu V, Conde J P, Freitas P P 2008 *J. Appl. Phys.* **103** 07E924
[77] Guedes A, Patil S B, Wisniowski P, Chu V, Conde J P, Freitas P P 2008 *IEEE Trans. Magn.* **44** 2554
[78] Hu J, Pan M, Tian W, Chen D, Zhao J, Luo F 2012 *Appl. Phys. Lett.* **100** 244102
[79] Du Q, Peng J, Qiu W, Ding Q, Pan M, Hu J, Sun K, Chen D, Pan L, Che Y, Zhang X, Li P, Zhang B 2019 *IEEE Electron Device Lett.* **40** 1824
[80] Pan L, Pan M, Hu J, Hu Y, Che Y, Yu Y, Wang N, Qiu W, Li P, Peng J, Jiang J 2020 *Sensors* **20** 1440
[81] Pan L, Hu J, Pan M, Che Y, Hu Y, Du Q, Sun K, Yu Y, Zhang Q, Peng J, Qiu W, Li P, Wang J 2021 *J. Magn. Magn. Mater.* **517** 167393
[82] Kanno A, Nakasato N, Oogane M, Fujiwara K, Nakano T, Arimoto T, Matsuzaki H, Ando Y 2022 *Sci. Rep.* **12** 6106
[83] Valadeiro J, Cardoso S, Macedo R, Guedes A, Gaspar J, Freitas P 2016 *Micromachines* **7** 88
[84] Zhang J, Pan M, Du Q, Hu J, Sun K, Yu Y, Zhang X, Luo H 2021 *Micromachines* **12** 722
[85] Kurashima K, Kataoka M, Nakano T, Fujiwara K, Kato S, Nakamura T, Yuzawa M, Masuda M, Ichimura K, Okatake S, Moriyasu Y, Sugiyama K, Oogane M, Ando Y, Kumagai S, Matsuzaki H, Mochizuki H 2023 *Sensors* **23** 646
[86] Dey C, Yari P, Wu K 2023 *Nano Futures* **7** 012002
[87] Murzin D, Mapps D J, Levada K, Belyaev V, Omelyanchik A, Panina L, Rodionova V 2020 *Sensors* **20** 1569
[88] Su D, Wu K, Saha R, Peng C, Wang J P 2019 *Micromachines* **11** 34
[89] An Z, Zhang L, Fan Y, Li Q, Li D 2025 *Sens. Actuators, A* **382** 116174
[90] Lu W S, You R, Zhou Y, Yuan H Y, You Z 2020 *Chin. J. Sci. Instrum.* **41** 1

[91] Ziegler P, Troster N, Schmidt D, Ruthardt J, Fischer M, Roth-Stielow J 2020 *2020 22nd European Conference on Power Electronics and Applications（EPE'20 ECCE Europe）* Lyon France, September 5–9, 2020 pP.1

[92] Liu J, Lee C K, Pong P W T 2024 *IEEE Trans. Instrum. Meas.* **73** 1

[93] Muehlenhoff C, Vogler C, Raberg W, Suess D, Albrecht M 2021 *IEEE Sensors J.* **21** 13176

[94] Yang L, Sun K, Pan M, Zhang X, Peng J, Hu Y, Hu J, Qiu W, Li P 2023 *IEEE Sensors J.* **23** 240

[95] Li R, Zhang S, Luo S, Guo Z, Xu Y, Ouyang J, Song M, Zou Q, Xi L, Yang X, Hong J, You L 2021 *Nat Electron* **4** 179

[96] Xu Y, Yang Y, Zhang M, Luo Z, Wu Y 2018 *Adv Mater. Technol.* **3** 1800073

[97] Shiogai J, Fujiwara K, Nojima T, Tsukazaki A 2021 *Commun. Mater.* **2** 102

[98] Camsari K Y, Torunbalci M M, Borders W A, Ohno H, Fukami S 2021 *Phys. Rev. Appl.* **15** 044049

[99] Krizakova V, Perumkunnil M, Couet S, Gambardella P, Garello K 2022 *J. Magn. Magn. Mater.* **562** 169692

[100] Finocchio G, Incorvia J A C, Friedman J S, Yang Q, Giordano A, Grollier J, Yang H, Ciubotaru F, Chumak A V, Naeemi A J, Cotofana S D, Tomasello R, Panagopoulos C, Carpentieri M, Lin P, Pan G, Yang J J, Todri-Sanial A, Boschetto G, Makasheva K, Sangwan V K, Trivedi A R, Hersam M C, Camsari K Y, McMahon P L, Datta S, Koiller B, Aguilar G H, Temporão G P, Rodrigues D R, Sunada S, Everschor-Sitte K, Tatsumura K, Goto H, Puliafito V, Åkerman J, Takesue H, Ventra M D, Pershin Y V, Mukhopadhyay S, Roy K, Ting Wang I-, Kang W, Zhu Y, Kaushik B K, Hasler J, Ganguly S, Ghosh A W, Levy W, Roychowdhury V, Bandyopadhyay S 2024 *Nano Futures* **8** 012001

[101] Shao Q, Wang Z, Zhou Y, Fukami S, Querlioz D, Chua L O 2025 *Npj Spintronics* **3** 16